NUKLEONIKA 2006;51(1):21–28

Dense Plasma Focus as a powerful source of monochromatic X-ray radiation

Alexander V. Dubrovsky,
Vladimir A. Gribkov,
Yurii P. Ivanov,
Lesław Karpiński,
Marina A. Orlova,
Vera M. Romanova,
Marek Scholz,
Igor V. Volobuev

Abstract A review of some experimental results obtained using the dense plasma focus (DPF) device PF-1000 is presented. The copper $K_{\alpha_{1,2}}$ radiation line generated by DPF in the case of device anode made of copper was the main object of this study. The predominance of this characteristic radiation over other kinds of radiation in the DPF X-ray spectrum is shown. A brief description of a new DPF 6.0 device as well as a radioenzymology experiment carried out within this device is presented.

Key words Dense Plasma Focus • X-ray generation • X-ray dosimetry • exposure dose • absorbed dose • radioenzymology

A. V. Dubrovsky✉
Moscow Physical Society,
53 Leninsky Pr., 119991 Moscow, Russia
and Institute for Theoretical and Experimental Physics,
25 B. Cheremushkinskaya Str., 117259 Moscow, Russia,
Tel.: +7 095 132 6656; Fax: +7 095 710 1431,
E-mail: adubrov@mail.ru

Yu. P. Ivanov
Moscow Physical Society,
53 Leninsky Pr., 119991 Moscow, Russia

V. A. Gribkov, M. Scholz, L. Karpiński
Institute of Plasma Physics and Laser Microfusion,
23 Hery Str., 01-497 Warsaw, Poland

V. M. Romanova, I. V. Volobuev
P. N. Lebedev Physical Institute,
Russian Academy of Sciences,
53 Leninsky Pr., 119991 Moscow, Russia

M. A. Orlova
M. V. Lomonosov Moscow State University,
1 Leninskie Gory Str., Bld. 3, Moscow 119899, Russia

Received: 25 August 2005
Accepted: 30 November 2005

Introduction

A dense plasma focus device (DPF) just from its discovery [5, 7] is known as a powerful pulse generator of X-ray radiation of a very broad spectrum. The DPF spectrum usually is considered as consisting of two ranges: soft X-rays ($E_\gamma \sim 1$ keV) and hard X-rays ($E_\gamma \geq 20$ keV). Soft X-ray resultant as hot plasma thermal luminescence is mainly used, at present, in nanolithography and micromachinery [1, 3]. Hard X-rays of DPF enables the device to compete with any kind of habitual pulse X-ray tube due to its properties [4].

DPF hard X-ray spectrum has a vague similarity to that of X-ray tube depending on the atomic number Z of the anode material. It is an aliasing of characteristic radiation from bremsstrahlung both caused by the impact of a strong relativistic electron beam (REB) upon the anode surface. The DPF hard X-ray difference from an X-ray tube is formed by the two factors: specific anode mould as well as specific REB spectrum. The atomic characteristic radiation becomes excited under the ionization of the inner atomic shell by an electron beam. This kind of radiation is presented by a highly intensive doublet Cu$K_{\alpha_{1,2}}$ in the spectrum of hard X-rays generated by DPF having a copper anode. The doublet is originated with a copper atom single ionization, when a single vacancy appears in the *K*-shell. The vacancy is filled up with the $L_{2,3}$-shell electron, so the doublet is appearing.

The DPF bremsstrahlung differs from the X-ray tube radiation by the lack of sharp edge in the short-

wave spectrum region. The maximal DPF radiation intensity is concentrated in the 20–60 keV interval, but its short-wave spectral part has a negative-going character and stretches up to 1 MeV.

DPF soft X-rays of the gamma-ray photon energy $E_\gamma \sim 1$ keV (that is typical of DPF mode of operation conditioned to lithography purposes and of hotspots generation mode [1, 3]) as well as DPF hard X-rays (with the exception of Cu$K_{\alpha_{1,2}}$ doublet) has a very sharp pulse generation time ($\tau \sim 10$–100 ns) and a very small source size ($d \sim 10$–100 μm). On the contrary, generation of the DPF radiation line of Cu$K_{\alpha_{1,2}}$ doublet, or better to say the Cu*K*-alpha radiation line, is more prolonged (probably $\tau \sim 0.1$–1.0 μs), while the source of this is more extensive in space ($d \sim 5$–100 mm). (Time as well as space limitation here is noted for different DPF devices separated on the energy store scale from 2 kJ to 1000 kJ.) A characteristic property of DPF X-ray radiation is an extremely high-energy share of *K*-alpha radiation line in the DPF common spectrum. A roughly estimated common spectrum of DPF X-rays is possible to imagine as it is shown in Fig. 2a. An interesting opportunity appears when a thin copper foil is used as a filter assigned to the leading-out DPF radiation from a vacuum chamber to the external space. When the copper filter thickness is in the range 0.01–0.10 mm, its absorption curve has some region of transparency near the so called *K*-edge. The existence of such a transparency region makes it possible to lead out through this one Cu*K*-alpha radiation line. But this filter is opaque for the radiation of different gamma-quanta energy hereabout to the named line (see Figs. 2b and 2c). This paper is devoted to the experimental study as well as to some application in radiobiology of the DPF Cu*K*-alpha radiation line.

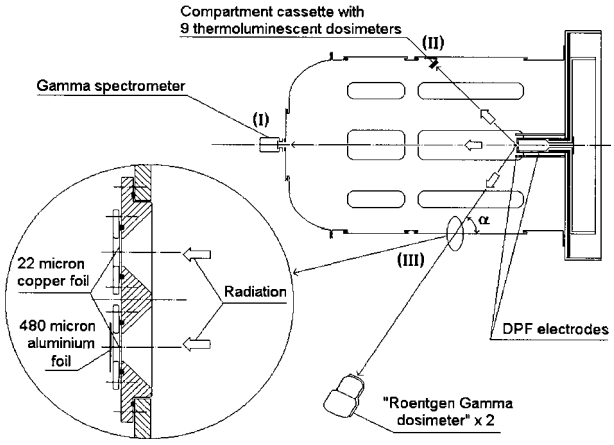

Fig. 1. Schematic sketch of PF-1000 experiment.

Experiments within PF-1000 device

Three experiments described below were carried out at different times. Since the experimental conditions were similar, so they are pictured on the same drawing (Fig. 1). The device was operated with bank capacity $C = 960$ μF, so the energy store was changeable from 175 kJ to 406 kJ through the variation of the charging voltage from 19 kV to 29.1 kV. Pure hydrogen under a pressure of 160–320 Pa was used as a working gas.

The first experiment ((I), Fig. 1), is X-ray spectrometry within the spectral region $E_\gamma \sim 7$–9 keV. The focusing spectrograph with a bidimensional spatial resolution (FSSR-2d) was used [9]. The spectrum obtained is presented in Fig. 3. The Cu$K_{\alpha_{1,2}}$ doublet is distinctly seen on the picture. Tabulated values of the

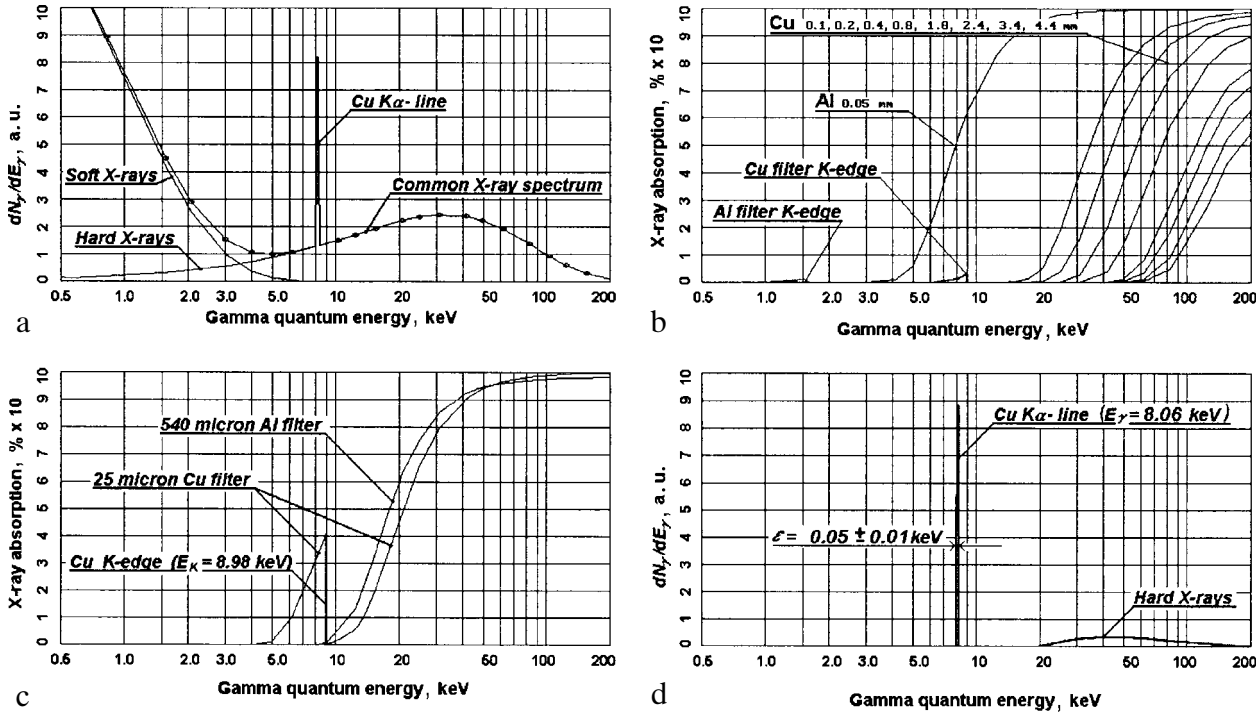

Fig. 2. a – A roughly estimated common spectrum of DPF X-ray; b – the 9 filters absorption curve family; c – two X-ray absorption curves; d – an approximate DPF X-ray spectrum behind thin (0.1 mm) copper filter.

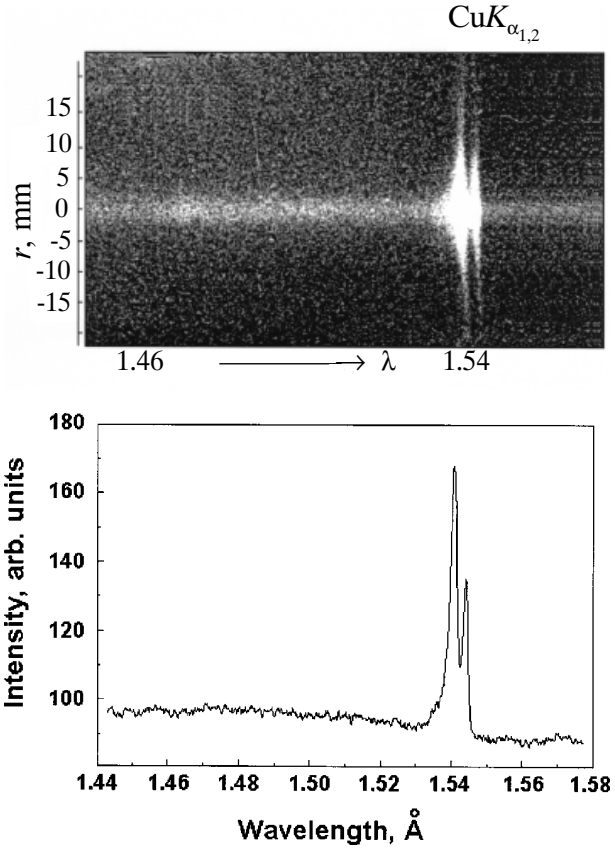

Fig. 3. DPF spectrum region containing Cu$K_{\alpha_{1,2}}$ doublet.

doublet lines are: λ_1 = 1.537 Å, λ_2 = 1.541 Å – or converting to kiloelectronvolts: E_{γ_1} = 8.068 keV, and E_{γ_2} = 8.047 keV. If one takes the doublet as a single line, it is rationally to assume E_γ = 8.06 keV for CuK_α. The experimentally measured half-width line is $\varepsilon = 0.05 \pm 0.01$ keV.

The experiment 2 ((II), Fig. 1), is the estimation of DPF X-ray spectrum by means of multi-channel thermoluminescence dosimetry. Nine lithium fluoride (LiF) tablets, which were used as TLD, have been located as unit inside the vacuum chamber of PF-1000 installation. Each tablet was put into its cell of the dosimeter-holder, which is a thin plate with 9 halls of the diameter D = 8 mm, just as the tablet diameter, equipped with a substrate. The dosimeter holder was covered with some combination of copper foil sheets, so that each of the 8 tablets turned out to be hidden by its own copper filter according to the enumeration presented in Fig. 2b. The cassette as unit was covered with a 50 mm aluminum foil. Two sets of TLD have been irradiated in two series of DPF shots, 10 shots each. Two month after, the irradiated TLD as well as the control ones (to determine background level) were processed. The result of the processing is presented in Table 1. The reading data are in Roentgen units (R). The standard background count was found as 18 R. The data presented in Table 1 were found by subtraction of the background value from those found experimentally.

The 9 filter absorption curve family is presented in Fig. 2b. An examination of tabular results together with filter curves enables to calculate unknown X-ray spectrum as a matter of principle. But in practice, when the experimental error of the TLD method is ± 10% (taking standard background value as 18, the short-wave data are comparable with that value, so the error is ± 100% on this spectral part) this problem is insolvable. On the other hand, if provisional data about the unknown spectrum is available, some speculation on the subject of spectral character is reasonable. Really, the spectrum proposed in Fig. 2d is in very good accordance with data in Table 1. The presented X-ray spectrum consists of two components: the CuK_α line and a bell-shaped curve corresponding to the hard X-rays. The transparency of the aluminum filter to the radiation line is 50%; the transparency of a 0.1 mm copper filter in the spectral range, close to the CuK-edge is about 3%. The rest of filters is absolutely opaque to the CuK_α radiation line, since for the filter of 0.2 mm and larger, the K-edge is not presented on the absorption curve. Another rough evaluation one can extract from the data in tables: the average energy generation in the form of CuK_α radiation per single shot was 4.7 J and 6.5 J in the 1st and 2nd series, correspondingly.

The third experiment within PF-1000 device was devoted to study the CuK_α radiation line ((III) Fig. 1). Two absolutely equal windows of 14 mm in diameter were vacuum-tightly closed up with 22 μm copper foils. Two roentgen-gamma dosimeters VA-J-15 produced by VEB RFT firm, Dresden, being the ion production chambers and well co-working with the electronics, were situated at a distance of 180 cm from the window, or 268 cm from the central point of the plasma focus anode. Each dosimeter was looking at the anode central point through its own window. The dosimeter registrations were read during the time of the PF-1000 device operation in two modes. A calibration mode consisted of data reading under the same conditions for the two dosimeters, i.e. a 22 μm Cu filter hides each one from the radiation source. This mode confirms the observational accuracy of measuring as ± 1.5%. At the time of working operation mode, one window was closed with an additional filter – a multilayer aluminum foil-set of 480 μm common thickness. The effect of the addition of such an insignificant filter as about 0.5 mm of pure

Table 1. The outcome of thermoluminescence dosimetry data processing

Filter (in mm)	0.05 Al	0.1 Cu +0.05 Al	0.2 Cu +0.05Al	0.4 Cu +0.05 Al	0.8 Cu +0.05 Al	1.8 Cu +0.05 Al	2.4 Cu +0.05 Al	3.4 Cu +0.05 Al	4.4 Cu +0.05 Al
1st measurement data, roentgen	4136	962	743	56	51	22	17	15	12
2nd measurement data, roentgen	5609	1001	155	103	14	8	6	5	4

Al was strange. The data read by the dosimeter closed with this additional filter shows a fall of more than an order of magnitude in comparison with the other dosimeter data.

The absorption curves of both filters are shown in Fig. 2c. The effective thickness of each filter is recounted as 25 μm and 540 μm taking into consideration the angle $\alpha = 63°$ (see Fig. 1). The results of measuring were processed in the following way. Let us name the data obtained as J_{Cu} and J_{Cu+Al}. The radiation dose behind the pure copper filter consists of two components: $J_{Cu} = J_{K\text{-alpha}} + J_{Hard}$; whereas that behind (Cu + Al) filter: $J_{Cu+Al} = \theta \cdot J_{Hard}$. Here θ is a reduction factor of J_{Hard} by the Al filter. From the Al filter, the absorption curve follows $\theta \approx 0.8$ for the spectral region 20–60 keV. So we have: $J_{Cu+Al} = 0.8 J_{Hard}$. Two values: $J_{K\text{-alpha}}$ and J_{Hard} – can be calculated as the two equations set roots.

The results obtained through two experimental series carried out within the PF-1000 device are presented in Figs. 4 and 5. The data given in Fig. 4 were obtained when the device was operated at a constant energy store level of $W = 300$ kJ. There were more or less fortunate shots within the series. Curve 1 illustrates a direct relation between $J_{K\text{-alpha}}$ and J_{Hard} radiation doses: the larger J_{Hard} dose – the larger $J_{K\text{-alpha}}$. But the ratio $J_{K\text{-alpha}}/J_{Hard}$ decreases with rising hard X-ray dose (curve 2 Fig. 4). By the way, this series had been stopped when after 22 shots the 22 μm Cu foil was broken concurrently in both windows.

The second experimental series consisted of 22 good shots, too. The charging voltage (hence the energy store also) was as variable parameter. The results of processing experimental data are presented as functions of the DPF energy store in Fig. 5. The curves presented demonstrate the fact that each DPF device of some different dimensions and design has its optimal energy store. The PF-1000 equipped with small dimension electrodes (not used now) shows 350 kJ as such an optimum. It is possible to estimate the radiation energy of DPF in two spectral ranges: CuK_α and hard X-rays 20–60 keV with an optimal energy store from the plasma focus region around the axis part of the anode to the outward hemisphere (2π). Taking into account that a 180 cm stratum of the ear separated device window from the dosimeter absorbs 88% of CuK_α radiation and

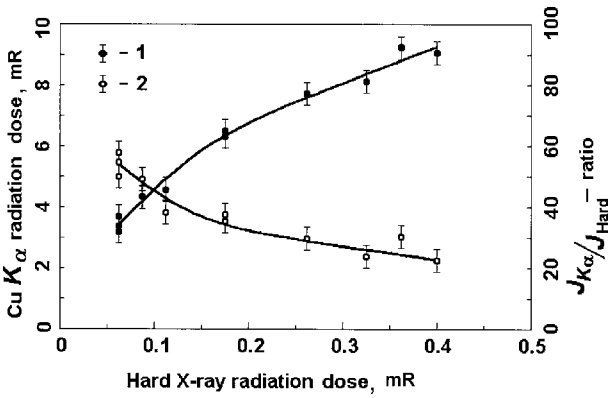

Fig. 4. Two experimental curves: 1 – CuK_α radiation dose vs. hard X-ray radiation dose; 2 – $J_{K\text{-alpha}}/J_{Hard}$ ratio subject to hard X-ray radiation dose (each plotted point has been calculated basing on data obtained on a certain DPF shot).

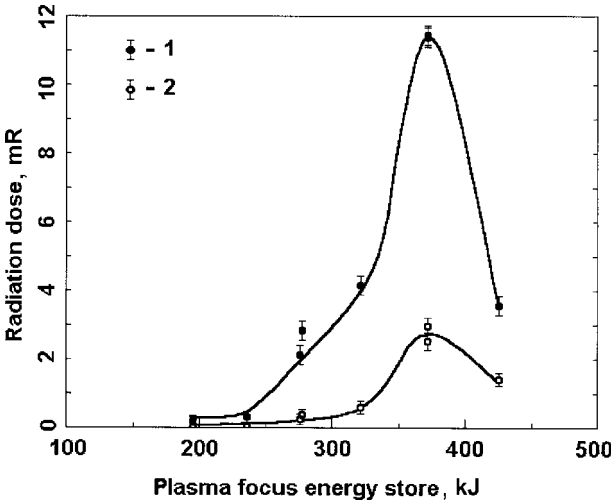

Fig. 5. Two experimental curves: 1 – CuK_α radiation dose; 2 – hard X-ray radiation dose subject to DPF energy store.

~ 5% of hard X-rays, and considering also the absorption energy by both filters (see Fig. 2c) one can get: $W_{K\text{-alpha}} = 0.10$ J; $W_{Hard} = 0.032$ J. Such unpretentious values are explained by the fact that the device anode has a reach-through opening of 3 cm in diameter in its central part. Plasma focus device optimized for the hard X-ray generation has generally a flat anode [3]. Such a characteristic property sharply increases the DPF X-ray radiation ability. A significant excess of previously described experimental result can probably be explained by the fact that TLD was situated inside the DPF chamber, so they collected radiation energy from the whole anode surface. On the contrary, each roentgen-gamma dosimeter was able to observe only a small central part of the anode.

DPF 6.0 device

Application of CuK_α radiation from the DPF device for goals in radiobiology has been undertaken by means of a recently initiated DPF 6.0 installation. Since the installation is not described in the literature as yet, we present here its brief description. The DPF 6.0 device was designed and realized as a result of joint operations of the IAEA RC No. 11942 and No. 11940 participators. It is situated at the Institute of Plasma Physics and Laser Microfusion (Warsaw, Poland). The main parameters of the DPF 6.0 installation are shown in Table 2. The installation is planned to be able to operate in the frequency regime. This condition noticeably has assigned its selection of elements. The electric circuit of the device is shown in Fig. 6. As it is well known now, any DPF device in spite of purely simplicity of its electric circuit is able to operate in an acceptable regime just in the case of an accurate selection of the circuit elements as well as of careful bus system realization. The DPF electric circuit includes high voltage capacitors, heavy-current switchboard, DPF chamber, current collector, and buses.

In order to realize required working conditions of the DPF-6.0 and to ensure the necessary DPF system

Table 2. General parameters of DPF 6.0 device

Battery capacity	28 μF
Actuating voltage	12–20 kV
Energy storage	2.0–7.0 kJ
DPF chamber type	exchangeable
Rep rate	1–10 Hz
Lifetime of the DPF system	more than 1 million shots

lifetime we have chosen high voltage capacitors of the type KMK 30-7 manufactured by Saint-Petersburg State Technical University (SPSTU) as a pilot production

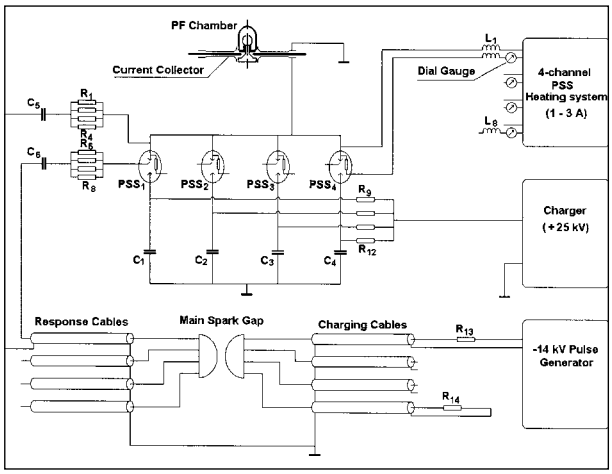

Fig. 6. Electric circuit of the DPF 6.0 device. The length of each charging as well as response coaxial cable is 6 m; R_1–R_8 = 100 Ω, 11 W; C_1–C_4 = 7 μF, 30 kV; C_5, C_6 = 66 pF, 30 kV; L_1–L_8 – high-voltage high-frequency noise protecting ferrite beads; R_{13} – charging resistor (single for the entire system); R_{14} – the resistor for cables discharge inter-shot.

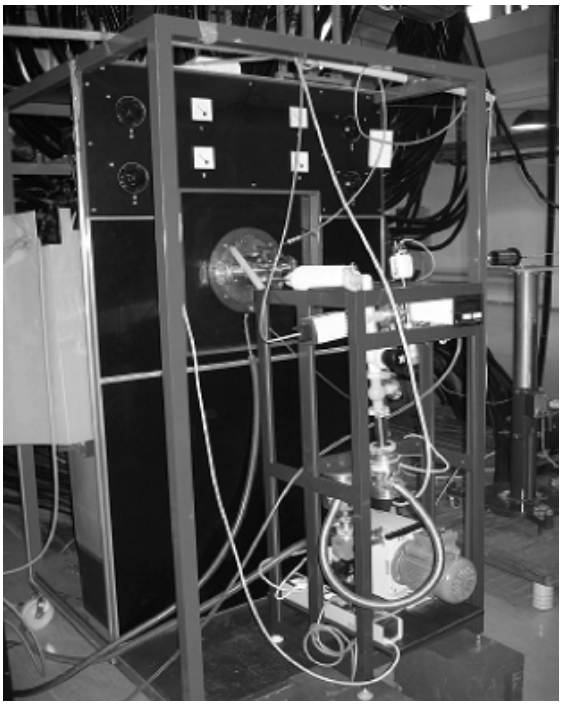

Fig. 7. The front view of DPF 6.0 device set.

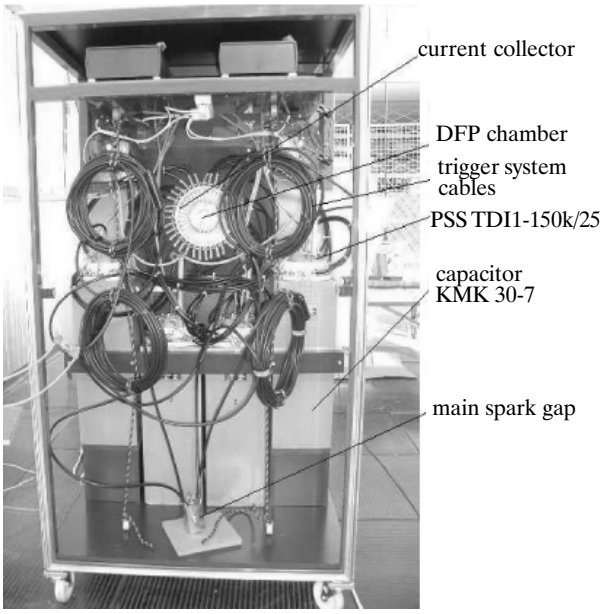

Fig. 8. The photo of DPF 6.0 device set.

with the following parameters: capacity C = 7 μF; nominal charging voltage V = 30 kV; inductance $L \le 10$ nH; short circuit current I_S = 350 kA. The pseudo-spark switcher TDI1-150k/25 elaborated and produced by the model shop "Pulse Technology Ltd", Ryazan, Russia we used as a current commutator. Some electrical parameters of the switch are: permissible anode voltage V_P = 25 kV; permissible current amplitude I_A = 200 kA; jitter t = 2 ns; permissible pulse frequency ν = 100 H.

Two photos of the DPF 6.0 device set are presented in Figs. 7 and 8. During the period 2004–2005, the device was operated after being completed with replaceable PF chambers of the three different types: neutron PF chamber, PF chamber of the open type, and hard X-ray PF chamber. In such a way three pilot experiments were carried out in regime of single shot. The rep rate regime is now infeasible because of lack of high voltage charger powerful enough. We describe here a hard X-ray experiment as bearing a direct relation to the main subject of this paper.

Dense Plasma Focus as a source of hard X-rays in radiation enzymology

The experiment described is a successive stage of a series of investigations carried out by the collaboration of physicists with biologists. The object of the investigation is a specific class of chemical agents so-called enzymes, which are very sensitive to radiation influence. In these experiments, different enzymes were irradiated *in vitro* with various doses, dose power, number of shots, and by various spectral ranges of the radiation. The biological samples irradiated in time short enough (some few hours) were studied analytically to register the behaviour of enzymes [6, 8].

The DPF hard X-ray chamber was used in experiments (Fig. 9). The design of this chamber we described in [2]. The hard X-ray chamber has a special insertion in

Fig. 9. The photo of hard X-ray DPF chamber.

the central part of the anode made of a high Z-number metal (W or Re) in order to raise the hard X-ray radiation intensity. However, the rest of the anode as well as the entire cathode of this chamber are made of pure, oxygen-free copper. As our experience testifies, the X-ray spectrum of such a chamber is as usually over-rich with the CuK_α radiation line. As indicated in the picture (Fig. 9), the chamber has two axisymmetrical windows. In our case, 100 μm copper foils closed both windows. So, we have again a combination of the CuK_α radiation with hard X-rays just as proposed in Fig. 2d. Now, let us look at the X-ray photo presented in Fig. 10, which has been prepared using the DPF described chamber. A personal dosimeter KID-2 is pictured on the photo. The bright round spot with heavy edge fuzziness is a result of K_α radiation influence on the X-ray film RT-5, hidden with black paper during the irradiation. On the contrary, the sharp image of the dosimeter insides is a result of the hard X-ray effect on the film. The dosimeter trunk is covered with a 1 mm aluminum shell, so it is absolutely opaque for CuK_α radiation. It is to note that the KID-2 dosimeter aluminum shell is detachable. More than one order of magnitude disparity between the dosimeter reading with or without the shell in the DPF experiment has been the first circumstance, which gives us a signal of the presence of CuK_α radiation material after Cu foil window. The X-ray photo (Fig. 10) demonstrates a very small hard X-ray source size, but, on the contrary, very lengthy dimensions of the CuK_α radiation source.

The idea of radiobiological experiment carried out within the DPF 6.0 device is to irradiate samples containing identical enzymes CuK_α X-rays of very wide dose range. The angular aperture of each out-window is 32°. Three small polyethylene test-tubes filled with an enzyme water-mixture were placed inside the conical irradiation zone not overshadowing each other at the distances: 23, 69, and 200 cm from the DPF window (experiment 1a, 1b, 1c, accordingly). Another experiment involves the irradiation of three test-tubes with different species of the enzyme mixture at a distance of 200 cm from DPF (experiment 2). The dose absorbed by each enzyme sample was calculated basing on the readings of the roentgen-gamma dosimeter, which was situated opposite to another DPF out-window at a distance of 11 cm from the filtered window to the dosimeter butt-end. The total distance from the source of radiation (the anode top surface) to the marked dosimeter mean level is 18.5 cm. The dosimeter readings according to the first and second experiments were: 11.4 mR and 19.4 mR, correspondingly. Taking into account the angular aperture of 32°, it is possible to consider the complete dosimeter working volume as being exposed to DPF radiation. So, the data presented were obtained in reliable measurements of the exposure dose at a distance of 18.5 cm from the source.

The last irradiated test-tube has been situated directly on the chamber window (3 cm from the source

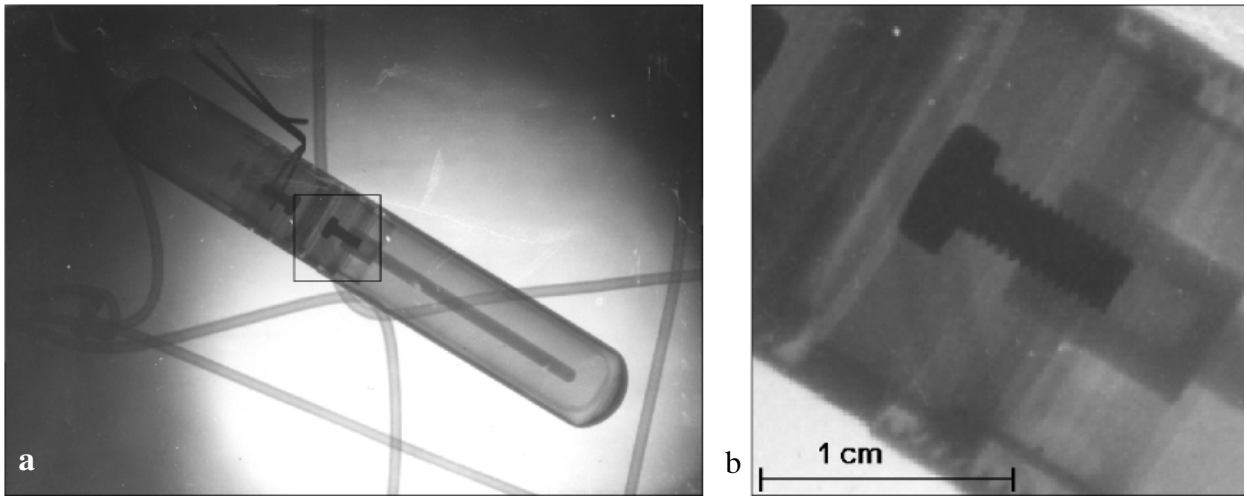

Fig. 10. The X-ray photo of KID-2 dosimeter attached to RT-5 X-ray film by the PVC pipe: a – general view; b – marked central fragment of the dosimeter.

to the bit core of tube). Three DPF shots have been produced. The dosimeter readings were: 10.3 mR, 25.0 mR, and 22.8 mR (experiment 3, the total exposure dose reading was 58.1 mR).

Discussion

Experimental results of biological analysis will be the subject of our next publications. This paper describes the experimental design as well as precise determination of the radiation dose absorbed by the test samples. Discussion of the obtained results is also presented.

So, the DPF device with a copper anode produces hard X-ray radiation which consists of two components: the CuK_α radiation line and the proper, hard X-rays. The DPF device functioning in an optimal operation regime generates energy which is divided between these two components at a 3:1 ratio (this not rigorously proven assumption relies on the results of our measurement carried out within a big PF-1000 device). The 1 mm aluminum filter commonly accepted in the X-ray engineering to leading-out hard X-rays from the Roentgen device, totally annihilates the CuK_α component. However, on applying a thin copper filter it is possible to lead out through this device a noticeable part of copper characteristic radiation. The X-ray dosimetry, as is well known, is not based on the determination of the X-ray energy transported through the dosimeter working medium, but it is based on the registration of the ionizing power of this radiation. The ionizing power of a CuK_α component, thanks to its position within the spectrum (E_γ = 8.06 keV), exceeds the component of another DPF radiation component (20 keV ≤ E_γ ≤ 60 keV). So, the difference between the dose readings separately obtained for each component is greater than 3/1. A similar appearance takes place in the irradiative experiment on DPF. The CuK_α radiation component produces the greatest contribution to the amount of absorbed energy by the sample. For example, a test-tube of a 10 mm in diameter filled with an enzyme water-mixture absorbs 100% of the CuK_α radiation energy, but only 25% of the hard X-ray component energy. On the other hand, the CuK_α component of DPF radiation endures a sizeable absorption in the ear as compared to the hard X-ray component, so the ratio between the exposure doses produced by the two named radiation components strongly changes its value as far as the distance from the source increases. A 200 cm layer of the ear, for example, allows to pass through 5.2% of CuK_α radiation, but the hard X-ray gating for the same stratum is 96%. This fact noticeably accrues to the $1/r^2$ functional dependence on the distance.

Taking into consideration the above cited, we have calculated the absorbed dose for each test tube containing enzymes irradiated within DPF 6.0 device. We make on assumption, which seems to us as most believable, that the ratio three to one takes place in the process of two components of radiation generated in the hard X-ray chamber. Consequently, we have:

1. Experiment 1:
   a) distance L = 23 cm, $D_{K\text{-alpha}}$ = 76.3 ± 0.3 μGy; D_{Hard} = 5.2 ± 0.9 μGy;
   b) distance L = 69 cm, $D_{K\text{-alpha}}$ = 4.25 ± 0.02 μGy; D_{Hard} = 0.57 ± 0.09 μGy;
   c) distance L = 200 cm, $D_{K\text{-alpha}}$ = 0.073 ± 0.003 μGy; D_{Hard} = 0.06 ± 0.01 μGy.
2. Two-component absorbed dose of each of three test samples (experiment 2) $D_{K\text{-alpha}}$ = 0.043 ± 0.002 μGy; D_{Hard} = 0.04 ± 0.01 μGy.
3. Experiment 3:
   distance L = 3 cm, $D_{K\text{-alpha}}$ = 16.2 ± 0.1 mGy; D_{Hard} = 3.1 ± 0.6 mGy.

It is to note that thanks to the fact that the CuK_α radiation is nearly monochromatic, thus the absorption as well as the definition of transmission coefficient is enough correct in this case. Thus, the calculation accuracy for this component is very good.

Conclusion

All of the described here experiments on the DPF device are in the unification by using a combination of copper anode with a thin copper filter, which is utilized for leading the X-ray radiation out of the device chamber. The presence of the transparency region near the *K*-edge on the copper absorption curve makes it possible to lead through this one characteristic Cu*K*-alpha radiation line. The portion of the radiation energy transported by the radiation line can be significant, as it has been shown in this paper.

It may be of interest to carry out an experiment utilizing some combination of anode-filter made of metal other than copper. This will give an opportunity to generate on the anode surface as well as to lead out of the chamber characteristic gamma-quanta of desirable energy. The list of possible metals suitable for such combinations is presented below

- Ti (*K*-alpha E_γ = 4.52 keV),
- Fe (*K*-alpha E_γ = 6.42 keV),
- Mo (*K*-alpha E_γ = 17.51 keV),
- Ag (*K*-alpha E_γ = 22.22 keV),
- W (*K*-alpha E_γ = 59.33 keV),
- Au (*K*-alpha E_γ = 68.89 keV).

Acknowledgment These works were supported in part by the International Atomic Energy Agency under the contracts No. 11940–11943, 12062.

References

1. Bogolyubov EP, Bochkov VD, Veretennikov VA *et al.* (1998) Powerful soft X-ray lithography based on plasma focusing. Phys Scripta 57:488–494
2. Dubrovsky AV, Gribkov VA, Ivanov YuP *et al.* (2001) 0.2-kJ and 2-kJ high rep rate Dense Plasma *foci*: their design, technology, and applications. Nukleonika 46;S1:s107–s111
3. Dubrovsky AV, Gribkov VA, Ivanov YuP, Lee S, Liu M (1999) Operation of a small dense plasma focus with neon gas filling in low and high pressure regimes. J Tech Phys 40:125–128
4. Dubrovsky AV, Silin PV, Gribkov VA, Volobuev IV (2000) DPF device application in the material characterization. Nukleonika 45;3:185–187

5. Filippov NV, Filippova TI, Vinogradov VP (1962) Dense high temperature plasma in a noncylindrical Z-pinch compression. Nucl Fusion S2:s77–s84
6. Gribkov VA, Orlova MA (2004) On various possibilities in pulsed radiation biochemistry and chemistry. Radiat Environ Bioph 43:303–309
7. Mather JW (1971) Dense plasma focus. In: Lovberg RH, Grien HR (eds) Method of experimental physics. Academic Press, London, pp 187–250
8. Orlova MA, Kost OA, Gribkov VA, Gazaryan IG, Dubrovsky AV, Egorov VA (2000) Enzyme activation and inactivation induced by low doses of irradiation. Appl Biochem Biotech 84:1–12
9. Skobelev IYu, Faenov AYa, Bryunetkin BA *et al*. (1995) Investigation of the emission properties of plasma structures with X-ray imaging spectroscopy. JETP 81;4:692–718